

Ultradrawing properties of ultra-high molecular weight polyethylene/hydrochloric acid treated attapulgite fibers

Jen-taut Yeh · Chuen-Kai Wang · Chih-Chen Tsai ·
Chih-Hsueh Lin · Chi-Yuan Huang · Kan-Nan Chen ·
Kuo-Shien Huang · Shih-Hsuan Chiu

Received: 23 January 2013 / Accepted: 8 August 2013 / Published online: 25 August 2013
© The Author(s) 2013. This article is published with open access at Springerlink.com

Abstract Investigation of the influence of the purified and acid treated attapulgite (ATP) contents on the ultradrawing properties of ultrahigh molecular weight polyethylene/purified attapulgites (UHMWPE/ATP, $F_{100}A_y$) and UHMWPE/acid treated ATP ($F_{100}A_{xM-y}$) as-prepared fibers is reported. In which, acid treated ATP nanofibers were treated with varying concentrations of hydrochloric solutions for various amounts of time. Similar to those found for the orientation factor values, the achievable draw ratios of the $F_{100}A_y$ and $F_{100}A_{xM-y}$ as-prepared fibers and tensile strength values of their drawn fibers approach a maximal value as their purified ATP and/or acid treated ATP

contents reach the optimal values at 0.05 and 0.025 wt%, respectively. In which, the maximal D_{ra} values of $F_{100}A_{xM-0.025}$ as-prepared series fiber specimens and the tensile strengths and moduli of the drawn $F_{100}A_{xM-0.025}$ fiber specimens are significantly higher than those of the $F_{100}A_{0.05}$ drawn fiber specimens prepared at the same draw ratios and optimal ATP contents but without acid treatment. Moreover, it is worth noting that the maximal D_{ra} values of the $F_{100}A_{xM-0.025}$ as-prepared fiber specimens and the tensile strengths and moduli of the drawn $F_{100}A_{xM-0.025}$ fiber specimens reached another maximal value as their ATP nanofibers were treated by 5 M HCl solutions for 60 min. To understand the interesting ultradrawing, orientation and tensile properties of $F_{100}A_y$ and $F_{100}A_{xM-y}$ fiber specimens, Fourier transform infra-red, specific surface areas, scanning electron microscope and elemental analyses of the purified and acid treated ATP nanofibers, and/or morphological and thermal analyses of the $F_{100}A_y$ and $F_{100}A_{xM-y}$ fiber specimens were performed in this study.

J.-t. Yeh (✉)

Hubei Collaborative Innovation Center for Advanced Organic Chemical Materials, Ministry of Education, Key Laboratory for the Green Preparation and Application of Functional Materials, Faculty of Materials Science and Engineering, Hubei University, Wuhan, China
e-mail: jyeh@mail.ntust.edu.tw

J.-t. Yeh · C.-K. Wang · C.-C. Tsai · C.-H. Lin · S.-H. Chiu
Graduate School of Material Science and Engineering, National Taiwan University of Science and Technology, Taipei, Taiwan

J.-t. Yeh

Key Laboratory of Green Processing and Functional Textiles of New Textile Materials, Wuhan University of Science and Engineering, Ministry of Education, Wuhan, China

J.-t. Yeh · K.-S. Huang

Department of Materials Engineering, Kun Shan University, Tainan, Taiwan

J.-t. Yeh

School of Printing and Packaging, Wuhan University, Wuhan, China

C.-Y. Huang

Department of Materials Engineering, Tatung University, Taipei, Taiwan

K.-N. Chen

Department of Chemistry, Tamkang University, New Taipei City, Taiwan

Keywords Ultradrawing · Attapulgite · Acid treatment · Ultrahigh molecular weight polyethylene

Introduction

Competition among high-performance fibers has prompted new processing methods for obtaining high-performance fibers of ultrahigh molecular weight polyethylene (UHMWPE) [1–11]. The key element in obtaining high-strength UHMWPE fibers is to find a way to draw the as-prepared gel specimens to an ultrahigh draw ratio after the gel spinning process. The drawability of the as-prepared gel specimens was found to depend significantly on the compositions of solutions from which gels were made [12–17]. Several authors [16, 18–22] reported that the drawing temperature and rate could markedly affect the maximal achievable draw ratio and tensile properties of solution-grown UHMWPE samples. In addition to the gel

solution compositions and drawing conditions, it is generally recognized that the conditions used in the formation process after spinning and/or solution casting of gel solutions can also have a significant influence on the morphology, microstructure and drawing properties of the specimens formed during the above mentioned processes [2, 19, 23–30].

The discovery of carbon nanotubes (CNTs) has attracted enormous attention in recent years due to their remarkable physical characteristics, such as, extremely high Young's modulus and rupture strength, high aspect ratio, nanometer-range diameter [25]. Presumably, incorporation of uniformly dispersed and aligned CNTs in polymer matrix can provide polymer composites with dramatically improved strength and modulus in their machine direction. These expectations have recently been confirmed by a number of studies [26–35]. Our recent investigation [32–34] found that the achievable draw ratios (D_{ra}) of UHMWPE/carbon nanotubes (CNTs) as-prepared fibers prepared near the optimal UHMWPE concentration improve consistently and reach a maximal value as their CNT and/or functionalized CNT contents increase up to an optimal value, respectively. As evidenced by DSC thermal analysis, CNTs with extremely high specific surface areas can serve as efficient nucleation sites and facilitate the crystallization of UHMWPE molecules into crystals but with low melting temperatures and/or evaluated smaller crystal thickness during their crystallization processes. Presumably, the crystals with lower melting temperatures and/or evaluated smaller crystal thickness obtained at proper plain and/or functionalized CNT contents can be melted and pulled out of folded lamellar crystals relatively easily during ultradrawing processes, and hence, results in higher drawability and orientation of the UHMWPE/CNTs or UHMWPE/functionalized CNTs as-prepared fibers. The ultimate tensile strength values of the UHMWPE/CNTs or UHMWPE/functionalized CNTs drawn fibers prepared using one-stage drawing process at 95 °C can reach 2.5 and 3.5 $GN m^{-2}$, respectively, which is about 17 and 66% higher than that of the corresponding plain UHMWPE drawn fibers prepared at the same optimal UHMWPE concentration and drawing condition but without CNTs.

Similar to CNTs, ATP is a natural clay mineral together with sepiolite that forms the group of fibrous clay minerals with extremely high specific surface areas ($\geq 200 m^2 g^{-1}$) [36–40]. Its structure scheme was firstly proposed by Bradly in 1940 [37], who described a theoretical formula of $(Mg, Al, Fe)_5Si_8O_{20}(Al)(HO)_2(OH)_4 \cdot 4H_2O$. In our recent study [41], natural and purified attapulgite (ATP) minerals were added in UHMWPE gel-spinning solutions to improve the ultradrawing and ultimate tensile properties of UHMWPE/ATPs fibers. Similar to those found for UHMWPE/CNTs or UHMWPE/functionalized CNTs as-prepared fibers, the achievable draw ratios of the UHMWPE/ATPs (FA_x) and UHMWPE/purified ATPs (FA_{mx}) as-prepared fibers and tensile strength values of their drawn fibers approach a maximal

value as their ATPs and/or purified ATPs contents reach the optimal values at 0.02 and 0.015 wt%, respectively. The maximal achievable draw ratios of FA_{mx} as-prepared series fiber specimens and the tensile strengths of the drawn FA_{mx} fiber specimens are significantly higher than those of the corresponding FA_x drawn fiber specimens prepared at the same draw ratios and ATPs contents but without purification by sodium hexametaphosphate. The ultimate tensile strength values of the UHMWPE/purified ATPs drawn fibers prepared at the optimal ATP content using one-stage drawing process at 95 °C can reach around 3.9 $GN m^{-2}$, which is even higher than most of those UHMWPE/functionalized CNTs drawn fibers prepared at the same drawing condition in our previous study [32–34, 41]. These results clearly suggest that nanofillers with extremely high specific surface areas can act as efficient nucleation sites and significantly improve the achievable draw ratios and ultimate tenacity properties of nanofillers added UHMWPE fibers.

In order to further improve the ultradrawing and ultimate tenacity properties of ATP added UHMWPE fibers, ATP nanofibers were etched by hydrochloric acid with varying concentrations for varying amounts of time to increase their specific surface areas in this study. The maximal achievable draw ratio obtained for each UHMWPE/acid treated ATP as-prepared fiber series specimens was significantly higher than that of the UHMWPE/purified ATP as-prepared fiber specimens prepared with the same optimal ATP content but without acid treatment. In which, the specific surface areas of ATP nanofibers were found to have a beneficial effect on the ultradrawing and ultimate tenacity properties of UHMWPE/acid treated ATP fibers. In order to understand the significantly improved ultradrawing and ultimate tenacity properties of the UHMWPE/acid treated ATP fibers, elemental, morphological and Fourier transform infrared analyses of the purified and acid treated ATP specimens and/or thermal, orientation factor, morphological and tensile properties of the as-prepared and drawn UHMWPE/purified ATP and UHMWPE/acid treated ATP fiber specimens were investigated.

Experimental

Materials and sample preparation

The UHMWPE resin and attapulgites (ATPs) used in this study were kindly supplied by Yung Chia Chemical Industrial Corporation, Kaohsiung, Taiwan and Xinyuan Science and Technology Corporation, Jiangsu, China, respectively, in which UHMWPE resin is associated with a weight-average molecular weight (Mw) of 5.0×10^6 . The ATP ore was first crushed by a hammer and then ground by a planetary ball mill (QM-ISPO4), which was manufactured by Nanjing University Instrument Plant, Nanjing, China. The ground ATP nanofibers

were firstly purified in sodium hexametaphosphate (SHMP) deionized water solutions under ultrasonic and stirring condition at 25 °C for 7 h, in which 20 g of ATP nanofibers together with 0.6 g of SHMP were dispersed and dissolved in 0.4 l of deionized water. Demarcated black impurity was found precipitating from the suspended upper layer solutions after setting the ultrasonic solutions still for half an hour. The suspended upper layer solutions were then centrifuged to remove impurities using a centrifuge model KDC-160HR for 15 min. The centrifuged ATP residue was dried at 80 °C for 24 h and then ground into purified ATP nanofibers using the planetary ball mill. Five grams of purified ATP nanofibers were treated with 100 ml of 1, 2, 3, 5 and 7 M hydrochloric acid (HCl) solutions under stirring condition at 70 °C for varying amounts of time, respectively. In which, 70 °C was chosen as the acid-treating temperature and used in the above experiments, since the acid treated ATP specimens treated with 3 M HCl solutions at 70 °C for 60 min exhibit significantly higher specific surface areas than those of acid treated ATP fibers treated with other temperatures for 60 min in our preliminary experiments. After treatment of HCl solutions, the ATP containing suspensions were filtered and washed with deionized water to neutral. The HCl treated ATP nanofibers were then dried at 80 °C for 24 h.

Varying compositions of purified or acid treated ATPs nanofibers together with UHMWPE resin were then dispersed and/or dissolved in decalin solvent at 135 °C for 1.5 h, in which 0.1 wt% of di-*t*-butyl-*p*-cresol was added as an antioxidant. The original and/or acid treated ATP nanofibers was dried at 80 °C for 24 h in a vacuum oven, before incorporation into the UHMWPE/ATP and/or UHMWPE/acid treated ATP gel solutions. The UHMWPE/ATP and/or UHMWPE/acid treated ATP gel solutions prepared above were then fed into a temperature-controlled hopper and kept as hot homogenized gel solutions before spinning. The hot homogenized gel solutions were then gel-spun using a conical die with an exit diameter of 1 mm at an extrusion rate of 1,000 mm/min and an extrusion temperature of 170 °C. A water bath and a winder with 70 mm in diameter were placed at a distance of 520 mm and 810 mm from the spinneret exit, respectively. The extruded gel fibers were cooled in a temperature-conditioned atmosphere and then quenched into a water bath for about 1 min, where the temperatures of the air atmosphere and water bath were controlled at 5 °C. The quenched fibers were then extracted in a n-hexane bath for 5 min to remove the residual decalin solvent. The extracted fiber specimens were then dried in air for 30 min to remove the remaining n-hexane solvent before any drawing run. Tables 1 and 2.

Morphological and elemental analysis

In order to understand the morphologies and elemental compositions on the surfaces of the purified and acid treated ATP

Table 1 Designations of purified and acid treated ATP specimens prepared in this study

Purified and acid treated attapulgitte specimens	Concentrations of hydrochloric acid solutions (M)
A	0
A _{1M}	1
A _{2M}	2
A _{3M}	3
A _{5M}	5
A _{7M}	7

Table 2 Designations and compositions of UHMWPE, UHMWPE/ATP and UHMWPE/acid treated ATP as-prepared fiber specimens

As-prepared fiber specimens	ATP (phr)	Acid treated ATP (phr)	UHMWPE (g)	Volumes of decalin in gel solutions (ml)
F ₁₀₀	0	0	100	5000
F _{100A_{0.0125}}	0.0125	–	100	5000
F _{100A_{0.025}}	0.025	–	100	5000
F _{100A_{0.05}}	0.05	–	100	5000
F _{100A_{0.15}}	0.15	–	100	5000
F _{100A_{0.25}}	0.25	–	100	5000
F _{100A_{1M-0.0125}}	–	0.0125	100	5000
F _{100A_{1M-0.025}}	–	0.025	100	5000
F _{100A_{1M-0.05}}	–	0.05	100	5000
F _{100A_{1M-0.15}}	–	0.15	100	5000
F _{100A_{1M-0.25}}	–	0.25	100	5000
F _{100A_{2M-0.0125}}	–	0.0125	100	5000
F _{100A_{2M-0.025}}	–	0.025	100	5000
F _{100A_{2M-0.05}}	–	0.05	100	5000
F _{100A_{2M-0.15}}	–	0.15	100	5000
F _{100A_{2M-0.25}}	–	0.25	100	5000
F _{100A_{3M-0.0125}}	–	0.0125	100	5000
F _{100A_{3M-0.025}}	–	0.025	100	5000
F _{100A_{3M-0.05}}	–	0.05	100	5000
F _{100A_{3M-0.15}}	–	0.15	100	5000
F _{100A_{3M-0.25}}	–	0.25	100	5000
F _{100A_{5M-0.0125}}	–	0.0125	100	5000
F _{100A_{5M-0.025}}	–	0.025	100	5000
F _{100A_{5M-0.05}}	–	0.05	100	5000
F _{100A_{5M-0.15}}	–	0.15	100	5000
F _{100A_{5M-0.25}}	–	0.25	100	5000
F _{100A_{7M-0.0125}}	–	0.0125	100	5000
F _{100A_{7M-0.025}}	–	0.025	100	5000
F _{100A_{7M-0.05}}	–	0.05	100	5000
F _{100A_{7M-0.15}}	–	0.15	100	5000
F _{100A_{7M-0.25}}	–	0.25	100	5000

nanofiber specimens prepared in “Materials and sample preparation” section. The original, purified and acid treated ATP nanofibers were dried at 80 °C for 24 h and then gold-coated at 15 keV for 10 s. The original, purified and acid treated ATP nanofibers were also dried and dispersed in alcohol and then dried onto a carbon-coated copper grid under ambient conditions prior to morphological and elemental analysis. A special accessory kit (attenuated total reflectance (ATR)) was used in elemental analysis to determine the content of light elements such as oxygen in original and/or acid treated ATP nanofibers. The UHMWPE, UHMWPE/purified ATP and UHMWPE/acid treated ATP as-prepared and drawn gel fibers were etched with excess amount of fuming nitric acid to highlight the crystalline morphology of the fiber specimen. The amorphous regions of fiber specimens could be etched with ultrasonic generator at 300 W at 60 °C. After the 6 h acid treatment the sample was washed subsequently by both de-ionized water by boiling acetone, and then dried at room temperature. The dried etched fiber specimens were then gold-coated at 15 keV for 10 s. The gold-coated ATP nanofiber and fiber specimens prepared above were then examined using a JEOL Field Emission Scanning Electron Microscope (FESEM) model JSM-6500 operated at 15 kV.

Specific surface area analysis

A Laser Particle Size Analyzer model BT-9300H (Dandong Bettersize Instruments Ltd., Dandong, China) was used to study the specific surface areas of the purified and acid treated ATP specimens prepared in the “Materials and sample preparation” section, although the specific surface areas of ATP and/or acid treated ATP fibers may be underestimated due to their porosity and surface roughness in feature. Before analysis, ten micrograms of purified and acid treated ATP nanofibers were added and ultrasonicated in 10 ml decalin at 25 °C for 5 min, respectively. The specific surface areas of purified and acid treated ATP specimens were then measured by placing the ultrasonicated solutions prepared above in the cuvette of the Laser Particle Size Analyzer at 25 °C.

Fourier transform infrared spectroscopy

Fourier transform infrared (FT-IR) spectroscopic measurements of the purified and acid treated ATP specimens were recorded on a Nicolet Avatar 360 FT-IR spectrophotometer at 25 °C, wherein 32 scans with a spectral resolution 1 cm⁻¹ were collected during each spectroscopic measurement. Infrared spectra of the film specimens were determined using the conventional KBr disk method. The original and modified ATP nanofibers were cast onto KBr disk and dried at 60 °C for 30 min. The cast films used in this study were prepared sufficiently thin enough to obey the Beer-Lambert law.

Thermal, lamellar thickness and orientation factor analysis

Thermal properties of all samples were performed on a TA differential scanning calorimeter (DSC) model Q100. All scans were carried out at a heating rate of 20 °C/min under flowing nitrogen at a flow rate of 25 ml/min. Samples weighing 0.5 mg and 15 mg were placed in the standard aluminum sample pans for determination of their melting temperature (T_m) and percentage crystallinity values, respectively. The percentage crystallinity values of the specimens were estimated using baselines drawn from 40 to 200 °C and a perfect heat of fusion of polyethylene of 293 J/g [42, 43].

In order to understand the ultradrawing properties of UHMWPE, UHMWPE/ATP and UHMWPE/acid treated ATP as-prepared fiber specimens, the lamellar thickness (l_c) values of the above as-prepared fibers were evaluated from their T_m values using Hoffman and Weeks' equation [43, 44] given as follows. Broad melting peak observed from non-isothermal DSC scans and the effect of lamella thickening may all lead to deviations from the true l_c values. Nevertheless, Hoffman-Weeks equation was used for qualitative estimation of l_c values of UHMWPE, UHMWPE/ATP and/or UHMWPE/acid treated ATP as-prepared fiber specimens, because it is the most feasible technique one can use to estimate the l_c values of fiber specimens. In which, an equilibrium melting temperature (T_m^0) of 145.5 °C, a perfect heat of fusion (ΔH_f^0) of 293 J/g and a folded surface free energy (σ_e) of 9×10^{-6} J/cm² of polyethylene crystals [43] were used for evaluation of l_c values of UHMWPE, UHMWPE/ATP and UHMWPE/acid treated ATP as-prepared fiber specimens.

$$T_m = T_m^0 \left[1 - \frac{2\sigma_e}{l_c \Delta H_f^0} \right] \quad (1)$$

The orientation factor (f_0) values of UHMWPE, UHMWPE/ATP and UHMWPE/acid treated ATP as-prepared and drawn fiber specimens were measured using a sonic velocity orientation instrument model SCY-III, which was purchased from Donghuakaili Chemicals and Fiber Technology Corporation, Shanghai, China. Before testing, the fiber specimen with 60 cm in length was wound and clamped on a testing device with a span of 40 cm. The f_0 values of the as-spun and drawn fiber specimens were then measured at 25 °C. A minimum of five samples of each specimen were tested and averaged during the orientation measurements. The f_0 values were evaluated using Eq. (2) as suggested by Xiao and coauthors [45]:

$$f_0 = 1 - (C_u/C)^2 \quad (2)$$

where C is the sonic velocity of the as-prepared or drawn UHMWPE fiber specimen and C_u is the sonic velocity of the fully unoriented sample, taken as 1.65 km/s [45].

Drawing and tensile properties of the fiber specimens

The UHMWPE, UHMWPE/ATP and UHMWPE/acid treated ATP fiber specimens used in the drawing experiments were cut from the dried as-prepared fibers and then stretched on a Gotech tension testing machine model GT-TFS-2000 equipped with a temperature-controlled oven. The fibers are 20 mm in length, which were wound and clamped in a stretching device and then stretched at 95 °C and a crosshead speed of 20 mm/min. The draw ratio of each fiber specimen was determined as the ratio of the marked displacement after and before drawing. The marked displacement before drawing was 27 mm. The tensile properties of the as-prepared and drawn fiber specimens were also determined using a Hung-Ta tension testing machine model HT-9112 at a crosshead speed of 20 mm/min. A minimum of five samples of each specimen were tested and averaged during the tensile experiments.

Results and Discussion

Morphological analyses of the original, purified and acid treated ATPs

Figure 1 exhibits typical SEM micrographs of original, purified and acid treated ATP specimens. Typical rodlike feature with dimensions of 150–600 nm in length and 10–45 nm in diameter was observed for original and purified ATP specimens. Before purification, the rodlike ATP nanofibers were found agglomerating and/or bundling together significantly on SEM micrograph of the original ATP specimen (see Fig. 1a). As shown in Fig 1b, the agglomerated bundles of ATP nanofibers originally present in original ATP specimen were significantly dispersed after the impurities were removed between ATP nanofibers. After acid treatment for a fixed amount of time, the surface roughness of acid treated ATP nanofibers seemed to increase due to hydrochloric acid etching even at low HCl concentrations, although agglomeration of ATP nanofibers was still present in acid-treated ATP specimens without ultrasonication. Moreover, the rodlike feature of ATP nanofibers were significantly etched into broken/shorter and thinner nanofibers by HCl solutions as their concentrations increase from 1 to 7 M (see Figs. 1c to g). In fact, after etching by 7 M HCl solution for 60 min, nearly only broken/short ATP nanofibers were found on the SEM micrograph of A_{7M} specimens (see Fig. 1g).

Figure 2 summarized typical SEM micrographs of A_{5M} specimens treated with 5 M HCl solution for various amounts of time. Similarly, after treating with 5 M HCl solutions, the rodlike feature of ATP nanofibers were etched into broken/shorter and thinner rodlike feature as the treating time increase from 20 to 100 min (see Fig. 2a to e). In fact, nearly only

broken and short ATP nanofibers were found on the SEM micrograph of A_{5M} specimens after they were excessive etched with 5 M HCl solutions for more than 60 min (see Fig. 2d to e).

Elemental analyses of the original, purified and acid treated ATPs

Table 3 summarized the compositions of original, purified and acid treated ATP specimens after elemental analyses. Elements, such as Si, Al and Mg were found [46] as the main compositions on the surfaces of original ATPs. The small amounts of P, Ca, Ni and Ti elements found on the surfaces of original ATPs are ascribed as the impurities that present as mineral compounds in the original ATPs, in which Ca element is reported present as CaCO₃ containing minerals [47]. After purification, the contents of Ca, Ni and Ti elements reduce significantly to 0.4, 0.6 and 0.3 wt%, respectively; but P contents increase from 0.5 to 4.3 wt%. Moreover, as shown in Table 4, Ca, Ni and Ti elements were indeed found as the main compositions of sediments after purification processes. These results suggest that Ca, Ni and Ti contained impurities originally present on the surfaces of ATP nanofibers precipitated as black sediments after their purification processes. During purification processes of ATP nanofibers, the abundant unbalanced charges present on surfaces of ATPs are likely to adsorb SHMP molecules with high P contents. As a consequence, Ni, Ti and Ca contained impurities reduce but P contained impurities increase significantly after the purification processes of ATP nanofibers.

After acid treatment for 60 min, the contents of P, Ni and Ti elements found on the surfaces of acid treated ATP nanofibers restore gradually to those contents found for the original ATP nanofibers, respectively, as the hydrochloric acid (HCl) concentrations used acid treatment increase from 1 to 7 M. In contrast, the contents of Ca element found on the surfaces of acid treated ATP specimens treated with HCl solutions for 60 min remain at low values 0.2 to 0.4 wt%, which are about the same as those found for the purified ATP specimens. As evidenced by morphological analyses in the previous section, after 60 min of acid treatment, the rodlike feature of ATP nanofibers were significantly etched into broken/shorter and/or thinner rodlike feature by HCl solutions as their concentrations increase from 1 to 7 M. These results clearly suggest that P, Ni and Ti elements originally present in ATP nanofibers gradually exposed after acid treatment for 60 min and P, Ni and Ti contents restored gradually to those found for purified ATP nanofibers, as the HCl concentrations used in the acid treatment increased from 1 to 7 M. The relatively low Ca contents found on the surfaces of acid treated ATP specimens is attributed to the easy dissolution of newly exposed CaCO₃ impurities in HCl solutions during the acid treating processes.

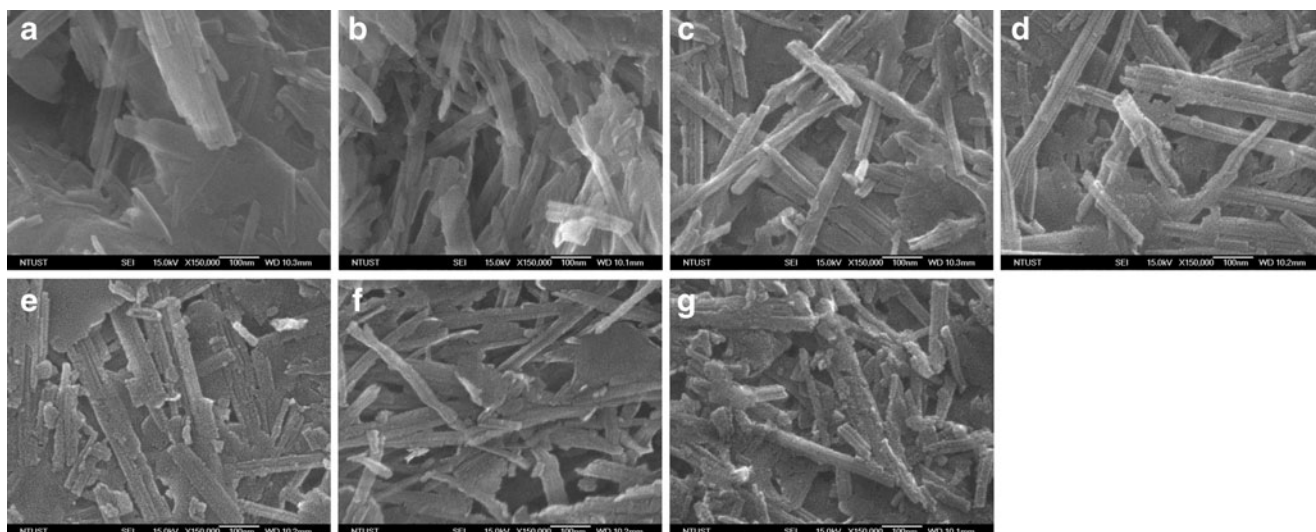


Fig. 1 SEM micrographs of **a** ATP, **b** purified ATP and **c** A_{1M}, **d** A_{2M}, **e** A_{3M}, **f** A_{5M} and **g** A_{7M} acid treated specimens treated with HCl solutions for 60 min

Specific surface area analyses

The values of specific surface areas of the purified and acid treated ATP nanofibers are summarized in Fig. 3. The specific surface area of the purified ATPs is relatively high and reaches 205 m²/g. After the treatment of HCl solutions, the specific surface areas of acid treated ATP nanofibers are significantly higher than those of the purified ATP nanofibers. In fact, the specific surface areas of each acid treated ATP nanofibers increase significantly with the increase in treating time, and then reach a maximal value as the treating time approaches an appropriate value around 60 min. The maximal specific surface areas obtained for acid treated ATP specimens reach another maximal value as the concentrations of HCl solutions

used for 60 min of acid treatment approach an optimal value at 5 M. As shown in Fig. 3, after treating ATP nanofibers in 5 M HCl solution for 60 min, the specific surface areas of the acid treated ATP nanofibers reaches around 282 m²/g, which is about 40 % higher than the specific surface area of purified ATP nanofibers without acid treatment. At HCl concentrations higher than 5 M or treating time more than the optimal value at 60 min, the specific surface areas of the acid treated ATP nanofibers reduce significantly with the further increase in the HCl concentration or treating time. For instance, the maximal specific surface areas of the ATP nanofibers acid-treated for an optimal amount of time at 60 min reduce from 282 m²/g to 250 m²/g, as the HCl concentrations increase from 5 M to 7 M. Similarly, the specific surface areas of ATP

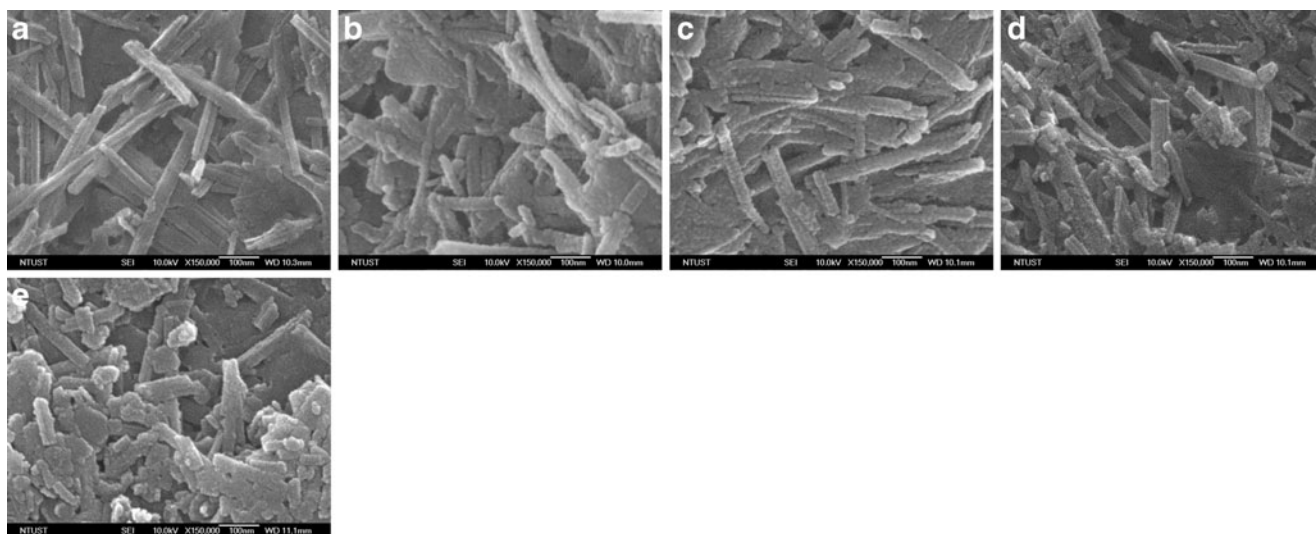


Fig. 2 SEM micrographs of acid treated ATP specimens after acid treatment with 5 M HCl solution for **a** 20, **b** 40, **c** 60, **d** 80, and **e** 100 min

Table 3 Elemental analyses of original, purified and acid treated ATP specimens

Compositions (wt%)	ATP	Purified ATP	A _{1M}	A _{2M}	A _{3M}	A _{5M}	A _{7M}
Si	62.5	62.4	62.4	62.3	62.4	62.5	62.3
Al	15.4	15.2	15.3	15.3	15.4	15.3	15.5
Mg	9.5	9.4	9.3	9.5	9.6	9.4	9.5
P	0.5	4.3	3.8	3.1	2.6	1.9	1.0
Ni	1.9	0.6	0.7	0.9	1.2	1.4	1.5
Ti	1.6	0.3	0.6	0.7	0.9	1.2	1.4
Ca	4.1	0.4	0.4	0.3	0.2	0.2	0.2

nanofibers treated with 5 M HCl concentration reduce from 282 m²/g to 275 m²/g, as the treating time increases from 60 to 80 min. As evidenced by morphological analysis in the previous section, the significant reduction in specific surface areas of acid treated ATP nanofibers with excessive treating time or HCl concentrations is attributed to the collapse of long ATP nanofibers originally with many free tunnels into significantly thinner and shorter ATP nanofibers with less free tunnels or cavities caused by over-etching of the HCl solutions.

Fourier transform infra-red spectroscopy

Figure 4 illustrates typical Fourier transform infra-red (FT-IR) spectra of original, purified and acid treated ATP specimens. As shown in the FT-IR spectrum of the original ATP specimen, seven distinguished absorption bands were found centering at 793, 882, 1,194, 1,433, 1,655, 3,582 and 3,616 cm⁻¹, which were generally ascribed to the motions of Ti-O bending, carbonate bending, Mg-O stretching, carbonate bending, absorbed water bending, Al-Mg-OH bending and Al₂-OH bending, respectively[41, 46]. After purification, the Ti-O and carbonate bending bands nearly disappeared, while demarcated Mg-O stretching, absorbed water bending, Al-Mg-OH bending and Al₂-OH bending bands were found centering at 1,195, 1,657, 3,583 and 3,616 cm⁻¹ of the FT-IR spectrum of purified ATP specimen (see Fig. 4b), respectively. Similar to those found for purified ATP specimen, demarcated Mg-O

Table 4 Elemental analyses of sediments after the purification processes of ATP specimens

Compositions (wt%)	Sediments
Si	0.05
Al	0.06
Mg	0.09
P	0.5
Ni	37.5
Ti	32.4
Ca	16.3

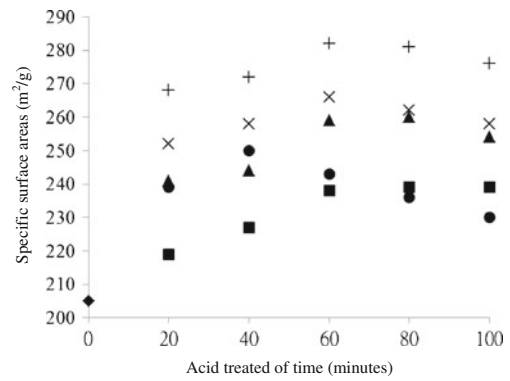


Fig. 3 Specific surface areas of A (♦), A_{1M} (■), A_{2M} (▲), A_{3M} (×), A_{5M} (+) and A_{7M} (●) specimens

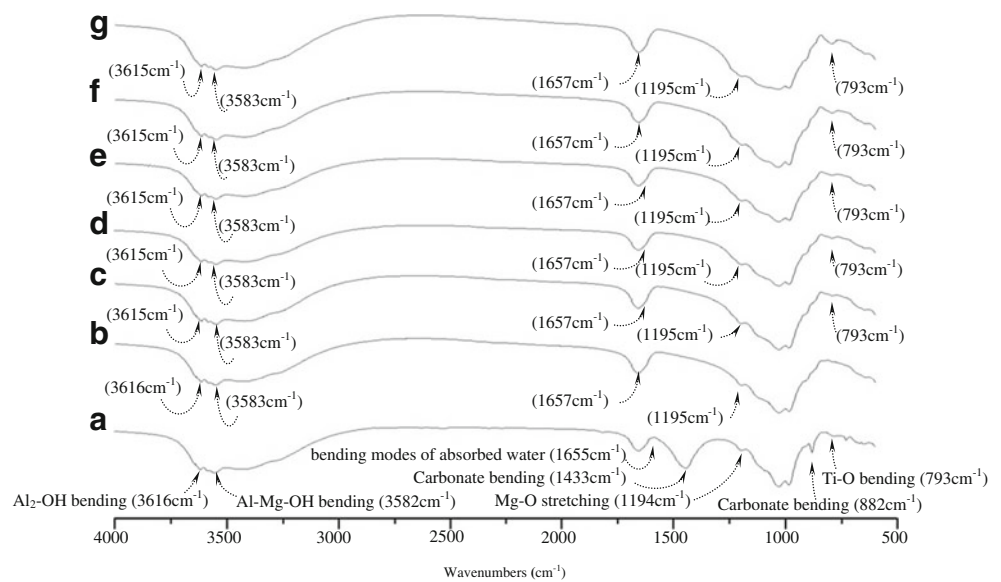
stretching, absorbed water bending, Al-Mg-OH bending and Al₂-OH bending bands were found centering at 1,195, 1,657, 3,583 and 3,615 cm⁻¹, respectively, of the FT-IR spectra of acid treated ATP specimen. However, Ti-O bending bands reappeared gradually and became more demarcated as HCl concentrations used for acid treatment increased from 1 to 7 M.

The disappearance of the Ti-O bending bands of purified ATP specimen is likely due to the adsorption of Ti²⁺ by SHMP after purification of ATP nanofibers. Whereas, the reappearance of Ti-O bending bands of acid treated ATP specimens is attributed to the newly exposed impurities containing Ti-O groups after acid treatment of purified ATP nanofibers. The disappearance of carbonate bending bands of the purified ATP specimens is most likely due to the adsorption of Ca²⁺ by SHMP after purification of ATP nanofibers, wherein CO₃²⁻ anions were combined with Na⁺ cations of SHMP to form Na₂CO₃ and then dissolved or precipitated in water. In contrast, the disappearance of carbonate bending bands of the acid treated ATP specimens is attributed to the easy dissolution of newly exposed CaCO₃ impurities in HCl solutions during the acid treating processes.

Thermal properties of the as-prepared fibers

Typical DSC thermograms of UHMWPE (F₁₀₀), UHMWPE/purified ATP (F₁₀₀A_y) and UHMWPE/acid treated ATP (F₁₀₀A_{xM-y}) as-prepared fiber series specimens are summarized in Figs. 5, 6, 7, 8, 9 and 10. Table 5 summarized the lamellar thickness (l_c) values of F₁₀₀, F₁₀₀A_y and F₁₀₀A_{xM-y} as-prepared fiber specimens evaluated from their melting temperature (T_m) values using Hoffman and Week's equation [43, 44]. A main melting endotherm with a peak melting temperature (T_m) and percentage crystallinity (X_c) at 139.6 °C and 65.3 %, respectively, was found for the F₁₀₀ as-prepared fiber specimen. The T_m(or evaluated l_c) and X_c values of F₁₀₀A_y and/or F₁₀₀A_{xM-y} as-prepared fiber series specimens approach the minimal and maximal values, as their purified and/or acid treated ATP approach the optimal values at 0.05 and 0.025 phr, respectively. In which, T_m(or evaluated l_c) and X_c values

Fig. 4 FT-IR spectra of the **a** original ATP, **b** A, **c** A_{1M}, **d** A_{2M}, **e** A_{3M}, **f** A_{5M} and **g** A_{7M} specimens



of the F₁₀₀A_{xM-y} as-prepared fiber specimens are significantly lower and higher than those of the corresponding F₁₀₀A_y as-prepared fiber specimens, respectively. For instance, T_m, l_c and X_c values of F₁₀₀A_{5M-0.025}/F₁₀₀A_{1M-0.05} as-prepared fiber specimen are 135.8 °C/137.4 °C, 9.6 nm/11.5 nm and 74.6 %/70.2 %, respectively, which are significantly lower than T_m and l_c values (i.e. 139.6 °C, 15.7 nm), but higher than X_c values (i.e. 65.3 %) of F₁₀₀ as-prepared fiber specimen. Moreover, it is worth noting that each F₁₀₀A_{5M-y} as-prepared fiber series specimen exhibits the lowest T_m (or evaluated l_c) but the highest X_c values among F₁₀₀A_{xM-y} as-prepared fiber series specimens with the same contents of acid treated ATP nanofibers treating with different HCl concentrations for 60 min (see Figs. 5, 6, 7, 8, 9 and 10). For instance, the T_m (or evaluated l_c) and X_c values of F₁₀₀A_{5M-0.025} as-prepared fiber are about 0.3 to 0.8 °C (or 0.3 to 0.9 nm) lower and 0.9 to 3.2 % higher than those of other corresponding F₁₀₀A_{xM-0.025}

as-prepared fiber specimens with the same contents of acid treated ATP nanofibers treating with HCl concentrations other than 5 M for 60 min.

As evidenced by the specific surface area and SEM analyses, the purified and acid treated ATP nanofibers are with relatively large surface areas per volume, which make them in close proximity to a large fraction of the UHMWPE matrix. Apparently, even small contents of purified and acid treated ATP nanofibers can serve as efficient nucleation sites for UHMWPE molecules during their gel-spinning processes. These efficient nucleation sites of purified and acid treated ATP nanofibers then facilitate the crystallization of UHMWPE molecules into crystals with thinner lamellar thickness and/or lower T_m values during their gel-spinning processes. Acid treated ATP nanofibers with even higher specific surface areas are likely to serve as more effective sites for nucleation of

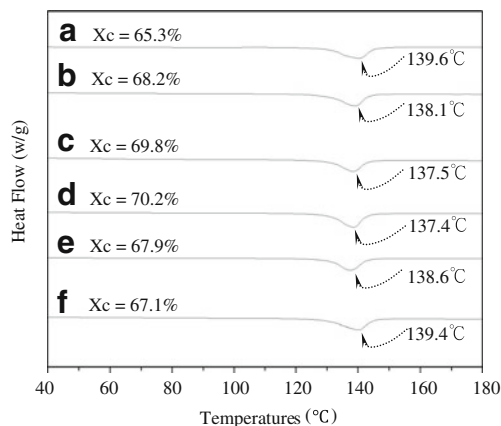


Fig. 5 DSC thermograms of **a** F100, **b** F100A0.0125, **c** F100A0.025, **d** F100A0.05, **e** F100A0.15, **f** F100A0.25 as-prepared fiber specimens

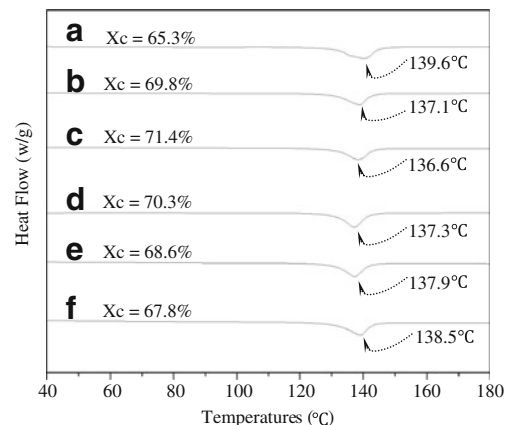


Fig. 6 DSC thermograms of **a** F100, **b** F100A1M-0.0125, **c** F100A1M-0.025, **d** F100A1M-0.05, **e** F100A1M-0.15, **f** F100A1M-0.25 as-prepared fiber specimens

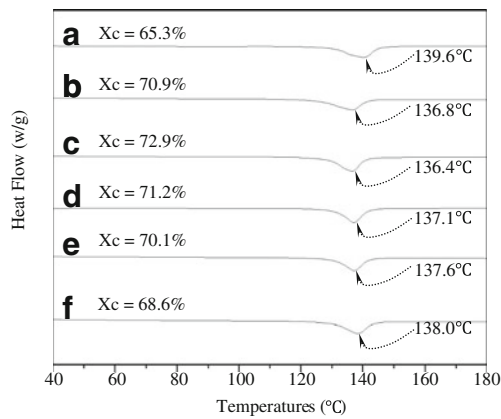


Fig. 7 DSC thermograms of **a** F100, **b** F100A2M-0.0125, **c** F100A2M-0.025, **d** F100A2M-0.05, **e** F100A2M-0.15, **f** F100A2M-0.25 as-prepared fiber specimens

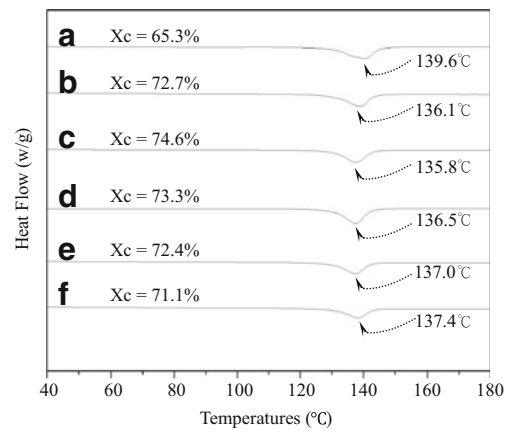


Fig. 9 DSC thermograms of **a** F100, **b** F100A5M-0.0125, **c** F100A5M-0.025, **d** F100A5M-0.05, **e** F100A5M-0.15, **f** F100A5M-0.25 as-prepared fiber specimens

UHMWPE molecules than purified ATP nanofibers. As a consequence, $F_{100}A_{5M-y}$ as-prepared fiber specimens exhibit significantly higher X_c but lower T_m and/or lamellar thickness values than the corresponding $F_{100}A_y$ and/or other $F_{100}A_{xM-y}$ as-prepared fiber specimens with the same purified and/or acid treated ATP contents, respectively.

Orientation factor

Typical orientation factor (f_o) values of F_{100} , $F_{100}A_y$ and $F_{100}A_{xM-y}$ as-prepared and drawn fiber series specimens are summarized in Fig. 11. No significant difference in f_o values was found for F_{100} , $F_{100}A_y$ and $F_{100}A_{xM-y}$ as-prepared fiber specimens. As expected, f_o values of F_{100} and each $F_{100}A_y$ or $F_{100}A_{xM-y}$ fiber series specimens increase consistently as their draw ratios increase. After addition of purified and/or acid treated ATP nanofibers, the f_o values of drawn $F_{100}A_y$ and/or $F_{100}A_{xM-y}$ fiber specimens are significantly higher than those

of F_{100} fiber specimens with the same draw ratios. The f_o values of drawn $F_{100}A_y$ and $F_{100}A_{xM-y}$ fiber specimens with the same draw ratios reach a maximal value as their purified and acid treated ATP contents approach the optimal values at 0.05 and 0.025 phr, respectively. In which, f_o values of drawn $F_{100}A_{xM-y}$ fiber specimens are higher than those of the corresponding $F_{100}A_y$ fiber specimens with the same draw ratios and ATP contents but without treating with HCl solutions. Furthermore, it is worth to note that the f_o values of drawn $F_{100}A_{xM-0.025}$ fiber specimens prepared at the optimal content of acid treated ATP nanofibers reach another maximal value as the HCl concentration and treating time approach the optimal value at 5 M and 60 min, respectively.

Achievable draw ratios of the as-prepared fiber specimens

Figure 12 summarized the achievable draw ratios (D_{ra}) of the F_{100} , $F_{100}A_y$ and $F_{100}A_{xM-y}$ as-prepared fibers prepared at

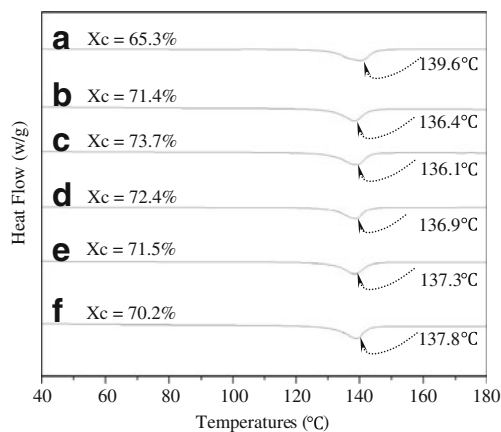


Fig. 8 DSC thermograms of **a** F100, **b** F100A3M-0.0125, **c** F100A3M-0.025, **d** F100A3M-0.05, **e** F100A3M-0.15, **f** F100A3M-0.25 as-prepared fiber specimens

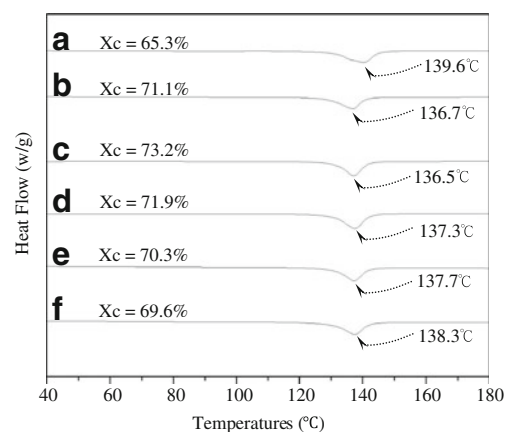


Fig. 10 DSC thermograms of **a** F100, **b** F100A7M-0.0125, **c** F100A7M-0.025, **d** F100A7M-0.05, **e** F100A7M-0.15, **f** F100A7M-0.25 as-prepared fiber specimens

Table 5 Melting temperatures and evaluated lamellar thickness values of UHMWPE as-prepared fiber specimens

Samples	T_m (°C)	σ_c (10^{-7} J/cm ²)	l_c (nm)
F ₁₀₀	139.6	90.0	15.7
F ₁₀₀ A _{0.0125}	138.1	90.0	12.6
F ₁₀₀ A _{0.025}	137.5	90.0	11.6
F ₁₀₀ A _{0.05}	137.4	90.0	11.5
F ₁₀₀ A _{0.15}	138.6	90.0	13.5
F ₁₀₀ A _{0.25}	139.4	90.0	15.2
F ₁₀₀ A _{1M-0.0125}	137.1	90.0	11.1
F ₁₀₀ A _{1M-0.025}	136.6	90.0	10.5
F ₁₀₀ A _{1M-0.05}	137.3	90.0	11.3
F ₁₀₀ A _{1M-0.15}	137.9	90.0	12.2
F ₁₀₀ A _{1M-0.25}	138.5	90.0	13.3
F ₁₀₀ A _{2M-0.0125}	136.8	90.0	10.7
F ₁₀₀ A _{2M-0.025}	136.4	90.0	10.2
F ₁₀₀ A _{2M-0.05}	137.1	90.0	11.1
F ₁₀₀ A _{2M-0.15}	137.6	90.0	11.8
F ₁₀₀ A _{2M-0.25}	138.0	90.0	12.4
F ₁₀₀ A _{3M-0.0125}	136.4	90.0	10.2
F ₁₀₀ A _{3M-0.025}	136.1	90.0	9.9
F ₁₀₀ A _{3M-0.05}	136.9	90.0	10.8
F ₁₀₀ A _{3M-0.15}	137.3	90.0	11.3
F ₁₀₀ A _{3M-0.25}	137.8	90.0	12.1
F ₁₀₀ A _{5M-0.0125}	136.1	90.0	9.9
F ₁₀₀ A _{5M-0.025}	135.8	90.0	9.6
F ₁₀₀ A _{5M-0.05}	136.5	90.0	10.3
F ₁₀₀ A _{5M-0.15}	137.0	90.0	10.9
F ₁₀₀ A _{5M-0.25}	137.4	90.0	11.5
F ₁₀₀ A _{7M-0.0125}	136.7	90.0	10.6
F ₁₀₀ A _{7M-0.025}	136.5	90.0	10.3
F ₁₀₀ A _{7M-0.05}	137.3	90.0	11.3
F ₁₀₀ A _{7M-0.15}	137.7	90.0	11.9
F ₁₀₀ A _{7M-0.25}	138.3	90.0	12.9

varying purified and acid treated ATP contents. Similar to those found in our previous study [41], D_{ra} values of $F_{100}A_y$ as-prepared fibers are significantly higher than that of the F_{100} as-prepared fiber specimen without addition of purified ATP nanofibers. The D_{ra} values of $F_{100}A_y$ as-prepared fiber series specimens increase significantly with the initial increase in purified ATP contents and then reach a maximal value at 145 as their purified ATP contents approach an optimal value at 0.05 phr. After treatment of HCl solutions on purified ATP nanofibers, the D_{ra} values of each $F_{100}A_{xM-y}$ as-prepared fiber series specimens are significantly higher than those of the corresponding $F_{100}A_y$ as-prepared fiber specimens with the same purified ATP contents but without acid treatment. Similar to those found for $F_{100}A_y$ as-prepared fiber specimens, the D_{ra} values of each $F_{100}A_{xM-y}$ as-prepared fiber series

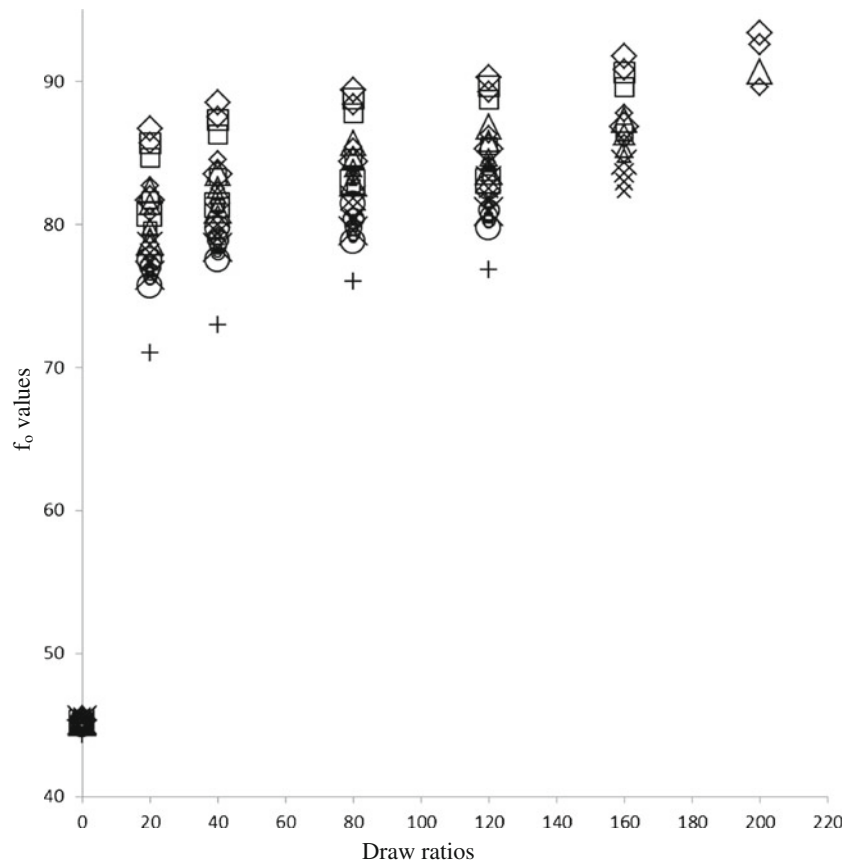
specimens reach a maximal value as their acid treated ATP contents approach a lower optimal value at 0.025 phr. Moreover, it is worth noting that the maximal D_{ra} values of the $F_{100}A_{xM-0.025}$ as-prepared fiber specimens reached another maximal value as their purified ATP nanofibers were treated by 5 M HCl solutions for 60 min. As shown in Fig. 12, the maximal D_{ra} values obtained for $F_{100}A_{5M-0.025}$ as-prepared fiber specimen reaches 249, which is significantly higher than those of $F_{100}A_{xM-0.025}$ as-prepared fiber specimens prepared with 0.025 phr ATP nanofibers treated with HCl concentrations other than 5 M.

As evidenced by thermal and lamellar thickness analyses, the T_m and/or evaluated l_c values of $F_{100}A_y$ and $F_{100}A_{xM-y}$ as-prepared fiber specimens reduce significantly with the increase in purified and/or acid treated ATP contents, although the amounts of crystals with lower T_m and/or evaluated l_c values increase significantly as their purified and/or acid treated ATP contents increase. Presumably, these crystals with lower T_m and/or evaluated l_c values obtained at higher purified and/or acid treated ATP contents can be melted and pulled out of folded lamellar crystals relatively easily during ultradrawing processes, and hence, results in higher drawability and orientation of the $F_{100}A_y$ and $F_{100}A_{xM-y}$ fibers. However, the amounts of coagulated and/or reticulated purified ATPs and/or acid treated ATPs are likely to increase significantly when their ATPs contents are higher than certain values. These coagulated and/or reticulated purified ATPs and/or acid treated ATPs can slide with each other and serve as the defects during the drawing processes of $F_{100}A_y$ and $F_{100}A_{xM-y}$ as-prepared fiber specimens. The defects are likely to hinder the drawing and orientation of crystallites of the ultradrawn fibers along the drawing direction, and hence lead to a significant reduction in their achievable draw ratio and orientation factor values. Based on these premises, it is reasonable to understand that the achievable draw ratios of $F_{100}A_y$ and $F_{100}A_{xM-y}$ as-prepared fiber specimens and orientation factor values of the $F_{100}A_y$ and $F_{100}A_{xM-y}$ fibers with a fixed draw ratio reduce significantly when their purified and/or acid treated ATP contents are higher than the specific optimal values.

Morphological analyses of the as-prepared and drawn fibers

Figure 13 show typical SEM micrographs of the as-prepared and drawn F_{100} , $F_{100}A_{0.025}$ or $F_{100}A_{5M-0.025}$ fiber specimens with various draw ratios. Many demarcated drawn “micro-fibrils” were found paralleling the drawing direction of the drawn F_{100} , $F_{100}A_{0.025}$ or $F_{100}A_{5M-0.025}$ fiber specimens as their draw ratios increase, wherein the thicknesses of these drawn micro-fibrils reduce significantly as the draw ratios increase. Moreover, it is worth noting that more and thinner “micro-fibrils” were found on the etched surfaces of $F_{100}A_{5M-0.025}$ fiber specimen than those of $F_{100}A_{0.025}$ and F_{100} fiber specimens with the same draw ratios, respectively.

Fig. 11 The orientation factor (f_o) values of F100 (+), F100A0.0125 (□), F100A0.025 (◇), F100A0.05 (△), F100A0.15 (×), F100A0.25 (○), F100A1M-0.0125 (□), F100A1M-0.025 (◇), F100A1M-0.05 (△), F100A1M-0.15 (×), F100A1M-0.25 (○), F100A2M-0.0125 (□), F100A2M-0.025 (◇), F100A2M-0.05 (△), F100A2M-0.15 (×), F100A2M-0.25 (○), F100A3M-0.0125 (□), F100A3M-0.025 (◇), F100A3M-0.05 (△), F100A3M-0.15 (×), F100A3M-0.25 (○), F100A5M-0.0125 (□), F100A5M-0.025 (◇), F100A5M-0.05 (△), F100A5M-0.15 (×), F100A5M-0.25 (○), F100A7M-0.0125 (□), F100A7M-0.025 (◇), F100A7M-0.05 (△), F100A7M-0.15 (×), F100A7M-0.25 (○) as-prepared and drawn fiber specimens with varying draw ratios



It is not completely clear what accounts for the interesting demarcated “micro-fibril” morphology found in the F_{100} , $F_{100}A_{0.025}$ or $F_{100}A_{5M-0.025}$ drawn fiber specimens. Presumably, during the ultra-drawing processes, many of the UHMWPE kebab crystals with relatively thinner lamellar thickness values can be unfolded and pulled out of the crystal lamellae in an easier way than those kebab crystals with thicker lamellar thickness values. The unfolded UHMWPE molecules pulled out from the kebab lamellae can then gradually transform into the oriented “micro-fibrils” during their

ultra-drawing processes. As evidenced by DSC analysis in the previous section, the T_m and/or evaluated l_c values of $F_{100}A_y$ and $F_{100}A_{xM-y}$ as-prepared fiber series specimens reduce significantly as their purified ATP and/or acid treated ATP contents increase. In which, crystals with rather low T_m and evaluated l_c values were found for $F_{100}A_{xM-y}$ fiber specimens than those of the corresponding $F_{100}A_y$ with the same ATP contents but without acid treatment. It is, therefore, reasonable to understand that the “micro-fibrils” found on the etched surfaces of drawn $F_{100}A_{5M-0.025}$ and $F_{100}A_{0.025}$ fiber specimens are more and thinner than those of the corresponding drawn F_{100} fiber specimens with the same draw ratios. In which, more and thinner “micro-fibrils” were found on the etched surfaces of $F_{100}A_{5M-0.025}$ fiber specimen than those of $F_{100}A_{0.025}$ and F_{100} fiber specimens with the same draw ratios.

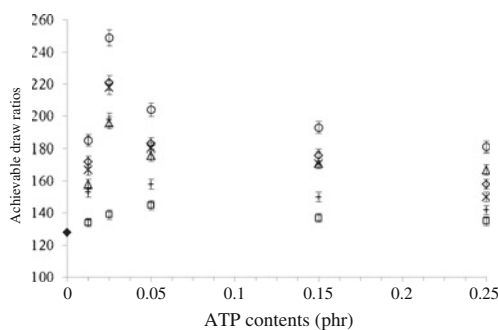
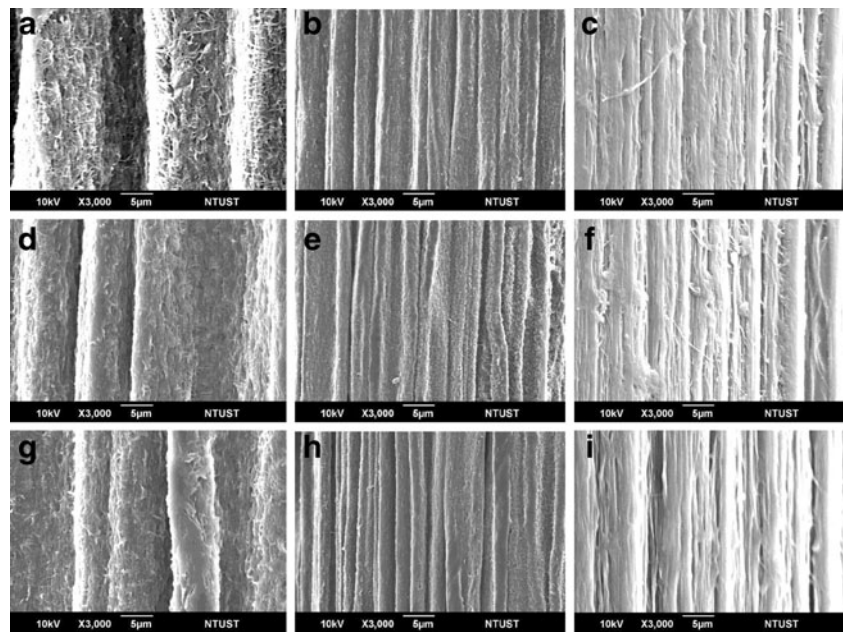


Fig. 12 Achievable draw ratios of F100 (◆), F100Ay (□), F100A1M-y (△), F100A2M-y (×), F100A3M-y (◇), F100A5M-y (○) and F100S7M-y (+) as-prepared fiber specimens

Tensile properties

The tensile properties of F_{100} , $F_{100}A_y$ and $F_{100}A_{xM-y}$ series fiber series specimens prepared at varying draw ratios are illustrated in Figs. 14 and 15 (Table 6). As expected, the tensile strength (σ_f) and modulus (E) values of the drawn F_{100} , $F_{100}A_y$ and $F_{100}A_{xM-y}$ fiber series specimens improve consistently as their draw ratios increase. Similar to those found for their orientation factors, the σ_f and E values of both

Fig. 13 SEM micrographs of the F100 fiber specimens with a draw ratio of **a** 1, **b** 50, **c** 100; and of the F100A0.025 fiber specimens with a draw ratio of **d** 1, **e** 50, **f** 100; and of the F100A5M-0.025 fiber specimens with a draw ratio of **g** 1, **h** 50, **i** 100



drawn $F_{100}A_y$ and $F_{100}A_{xM-y}$ fiber series specimens with a fixed draw ratio reach a maximal value as their purified and/or acid treated ATP contents approach the optimal values at 0.05 and 0.025 phr, respectively, wherein the σ_f and E values of the

$F_{100}A_{xM-y}$ fiber specimens are always significantly higher than those of the corresponding $F_{100}A_y$ fiber specimens prepared at the same draw ratios and ATP contents but without acid treatment.

Fig. 14 The tensile strength values of F100 (+), F100A0.0125 (□), F100A0.025 (◇), F100A0.05 (△), F100A0.15 (×), F100A0.25 (○), F100A1M-0.0125 (□), F100A1M-0.025 (◇), F100A1M-0.05 (△), F100A1M-0.15 (×), F100A1M-0.25 (○), F100A2M-0.0125 (□), F100A2M-0.025 (◇), F100A2M-0.05 (△), F100A2M-0.15 (×), F100A2M-0.25 (○), F100A3M-0.0125 (□), F100A3M-0.025 (◇), F100A3M-0.05 (△), F100A3M-0.15 (×), F100A3M-0.25 (○), F100A5M-0.0125 (□), F100A5M-0.025 (◇), F100A5M-0.05 (△), F100A5M-0.15 (×), F100A5M-0.25 (○), F100A7M-0.0125 (□), F100A7M-0.025 (◇), F100A7M-0.05 (△), F100A7M-0.15 (×), F100A7M-0.25 (○) fiber specimens with varying draw ratios

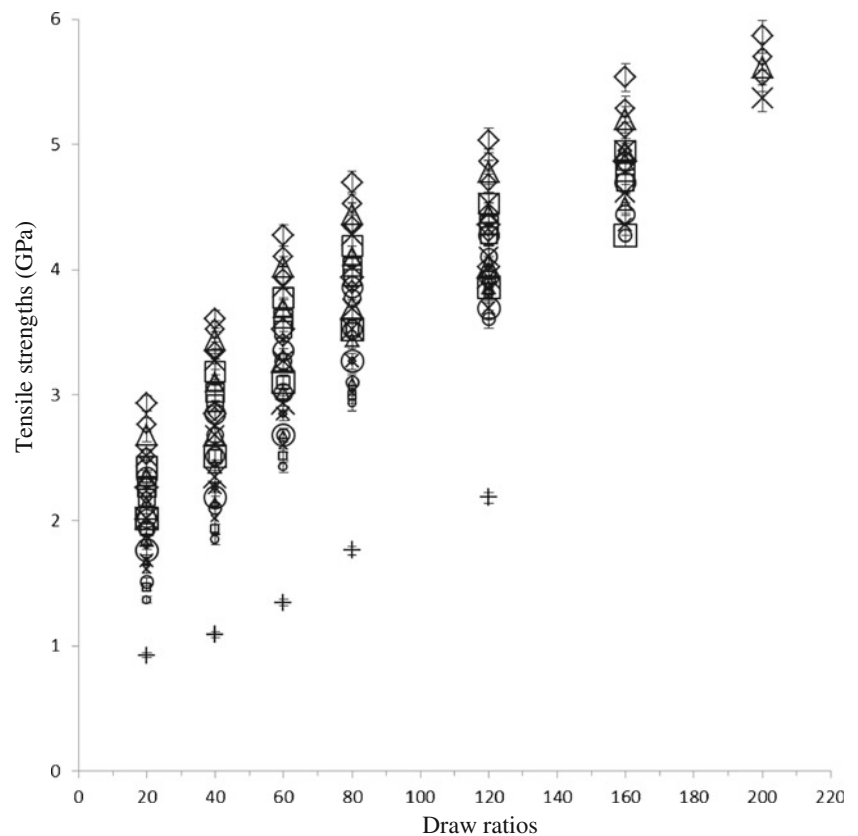
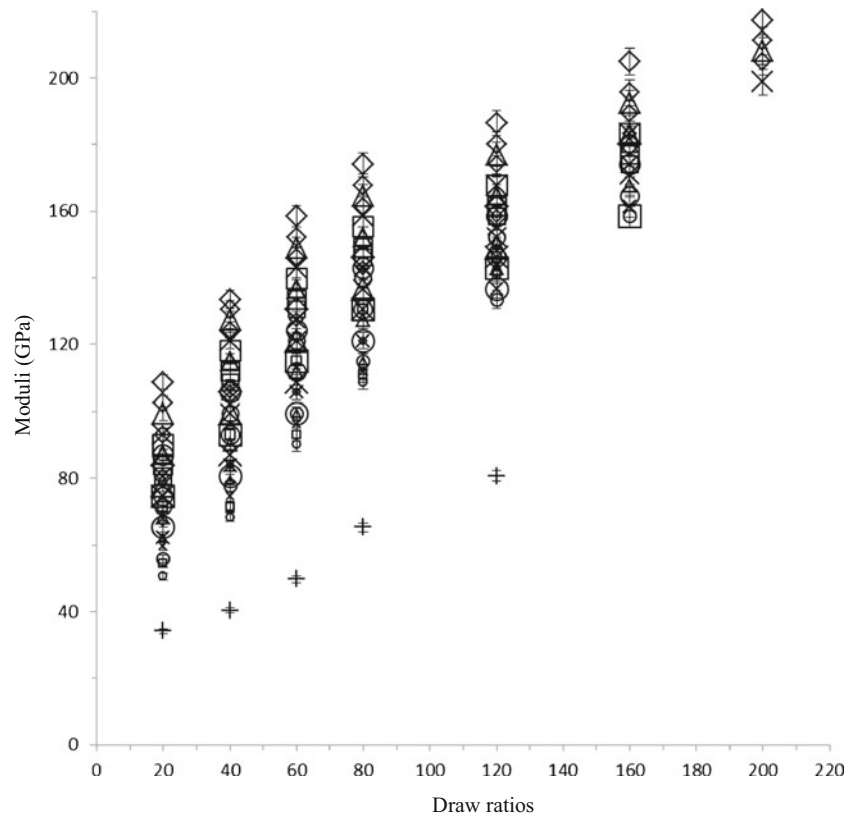


Fig. 15 The modulus values of F100 (+), F100A0.0125 (□), F100A0.025 (◇), F100A0.05 (△), F100A0.15 (×), F100A0.25 (○), F100A1M-0.0125 (□), F100A1M-0.025 (◇), F100A1M-0.05 (△), F100A1M-0.15 (×), F100A1M-0.25 (○), F100A2M-0.0125 (□), F100A2M-0.025 (◇), F100A2M-0.05 (△), F100A2M-0.15 (×), F100A2M-0.25 (○), F100A3M-0.0125 (□), F100A3M-0.025 (◇), F100A3M-0.05 (△), F100A3M-0.15 (×), F100A3M-0.25 (○), F100A5M-0.0125 (□), F100A5M-0.025 (◇), F100A5M-0.05 (△), F100A5M-0.15 (×), F100A5M-0.25 (○), F100A7M-0.0125 (□), F100A7M-0.025 (◇), F100A7M-0.05 (△), F100A7M-0.15 (×), F100A7M-0.25 (○) fiber specimens with varying draw ratios



The mechanical properties of the drawn specimens are generally believed to depend mainly on the degree of orientation of the drawn specimens, as their molecular weights are constant [48, 49]. As evidenced by the orientation analysis, at a fixed draw ratio, the orientation factor values of the drawn $F_{100}A_{0.05}$ and $F_{100}A_{xM-0.025}$ fiber specimens prepared at the optimal purified and acid treated ATP contents are always higher than those of other $F_{100}A_y$ and/or $F_{100}A_{xM-y}$ fiber specimens prepared at ATP and/or acid treated ATP contents deviating from their optimal values, respectively. In which, the orientation factor values of the $F_{100}A_{xM-0.025}$ fiber specimens are always higher than those of the corresponding $F_{100}A_{0.05}$ fiber specimens with the same draw ratios and ATP contents but without acid treatment. These results clearly suggest that a good orientation of UHMWPE molecules along the drawing direction positively affects the tensile properties of the $F_{100}A_y$ and $F_{100}A_{xM-y}$ fibers. Excellent orientation and tensile properties of the UHMWPE fibers can be prepared by ultradrawing the $F_{100}A_{0.05}$ and $F_{100}A_{xM-0.025}$ as-prepared fibers prepared at the optimal purified and/or acid treated ATP contents, respectively, in which, significant better orientation and tensile properties can be obtained for $F_{100}A_{xM-0.025}$ fiber specimens with even higher specific surface areas of acid treated ATP nanofibers.

Conclusions

The rodlike feature of acid treated ATP nanofibers were significantly etched into broken/shorter and thinner nanofibers by HCl solutions as their concentrations increase. In fact, after etching by 7 M HCl solution for 60 min, nearly only broken/short ATP nanofibers were found for A_{7M} specimen. Similarly, A_{5M} specimens were etched into broken/shorter and thinner rodlike feature as the treating time increased from 20 to 100 min. In which, nearly only broken and short ATP nanofibers were found for A_{5M} specimens after they were excessive etched for more than 60 min. The specific surface area of the purified ATP specimen is relatively high at 205 m^2/g . The specific surface areas of each acid treated ATP series specimens reach a maximal value as the treating time approaches an appropriate value at 60 min. The maximal specific surface areas obtained for acid treated ATP specimens reach another maximal value at 282 m^2/g as the HCl concentrations used for 60 min of acid treatment approach an optimal value at 5 M. The T_m (or evaluated l_c) and X_c values of $F_{100}A_y$ and/or $F_{100}A_{xM-y}$ as-prepared fiber series specimens approach the minimal and maximal values, as their purified and/or acid treated ATP approach the optimal values at 0.05 and 0.025 phr, respectively. In which, T_m (or evaluated l_c) and X_c values of the $F_{100}A_{xM-y}$ as-prepared fiber specimens are significantly lower and higher

Table 6 Tensile strength (σ_f) and modulus values (E) of UHMWPE drawn fiber specimens

Specimen	F ₁₀₀		F ₁₀₀ A _{0.0125}		F ₁₀₀ A _{0.025}		F ₁₀₀ A _{0.25}		F ₁₀₀ A _{1M-0.0125}	
	σ_f (GPa)	E(GPa)	σ_f (GPa)	E(GPa)	σ_f (GPa)	E(GPa)	σ_f (GPa)	E(GPa)	σ_f (GPa)	E(GPa)
20	0.9	34.2	1.5	54.3	1.8	66.8	1.4	50.6	1.9	71.4
40	1.1	40.4	1.9	71.4	2.3	83.8	1.8	68.3	2.5	93.2
60	1.3	49.7	2.5	93.2	2.9	105.6	2.4	90.1	3.1	114.9
120	2.2	80.7	3.8	141.0	4.0	149.1	3.8	141.6	3.9	146.0
	F ₁₀₀ A _{1M-0.025}		F ₁₀₀ A _{1M-0.25}		F ₁₀₀ A _{2M-0.0125}		F ₁₀₀ A _{2M-0.025}		F ₁₀₀ A _{2M-0.25}	
	σ_f (GPa)	E(GPa)	σ_f (GPa)	E(GPa)	σ_f (GPa)	E(GPa)	σ_f (GPa)	E(GPa)	σ_f (GPa)	E(GPa)
20	2.2	80.7	1.5	55.9	2.2	80.7	2.5	93.2	1.9	71.4
40	2.9	105.6	2.1	77.6	2.9	108.7	3.4	124.2	2.7	99.4
60	3.4	127.3	2.7	99.4	3.5	130.4	3.9	146.0	3.3	121.1
120	4.3	158.4	3.6	133.5	4.3	158.4	4.7	173.9	4.1	152.2
160	4.9	183.2	4.3	158.4	4.7	173.9	5.1	189.4	–	–
	F ₁₀₀ A _{3M-0.0125}		F ₁₀₀ A _{3M-0.025}		F ₁₀₀ A _{3M-0.25}		F ₁₀₀ A _{5M-0.0125}		F ₁₀₀ A _{5M-0.025}	
	σ_f (GPa)	E(GPa)	σ_f (GPa)	E(GPa)	σ_f (GPa)	E(GPa)	σ_f (GPa)	E(GPa)	σ_f (GPa)	E(GPa)
20	2.3	83.8	2.8	102.5	2.0	74.5	2.4	90.1	2.9	108.7
40	3.0	111.8	3.5	130.4	2.5	93.2	3.2	118.0	3.6	133.5
60	3.6	133.5	4.1	152.2	3.0	111.8	3.8	139.7	4.3	158.4
120	4.4	161.5	4.9	180.1	3.9	146.0	4.5	167.7	5.0	186.3
160	4.8	177.0	5.3	195.6	4.4	164.6	4.9	183.2	5.5	205.0
	F ₁₀₀ A _{5M-0.25}		F ₁₀₀ A _{7M-0.0125}		F ₁₀₀ A _{7M-0.025}		F ₁₀₀ A _{7M-0.25}		–	
	σ_f (GPa)	E(GPa)	σ_f (GPa)	E(GPa)	σ_f (GPa)	E(GPa)	σ_f (GPa)	E(GPa)	–	
20	2.3	87.0	2.0	74.5	2.3	83.8	1.8	65.2	–	
40	2.9	105.6	2.5	93.2	2.9	105.6	2.2	80.7	–	
60	3.4	124.2	3.1	114.9	3.5	130.4	2.7	99.4	–	
120	4.3	158.4	3.9	142.9	4.4	161.5	3.7	136.6	–	
160	4.7	173.9	4.3	158.4	4.9	180.1	–	–	–	

than those of the corresponding F₁₀₀A_y as-prepared fiber specimens with the same ATP contents but without acid treatment, respectively. Moreover, it is worth noting that each F₁₀₀A_{5M-y} as-prepared fiber series specimen exhibits the lowest T_m (or evaluated I_c) but the highest X_c values among F₁₀₀A_{xM-y} as-prepared fiber series specimens with the same contents of acid treated ATP nanofibers treating with different HCl concentrations for 60 min. Apparently, the efficient nucleation sites of purified and acid treated ATP nanofibers facilitate the crystallization of UHMWPE molecules into crystals with lower T_m (or evaluated I_c) values during their gel-spinning processes. Acid treated ATP nanofibers with higher specific surface areas appear to serve as more effective sites for nucleation of UHMWPE molecules than purified ATP nanofibers.

In a way similar to those found for the orientation factor values, the achievable draw ratios of the F₁₀₀A_y and F₁₀₀A_{xM-y} as-prepared fibers and tensile strength values of their drawn fibers approach a maximal value as their purified ATP and/or acid treated ATP contents reach the optimal

values at 0.05 and 0.025 wt%, respectively. The maximal D_{ra} values of F₁₀₀A_{xM-0.025} as-prepared series fiber specimens and the tensile strengths and moduli of the drawn F₁₀₀A_{xM-0.025} fiber specimens are significantly higher than those of the F₁₀₀A_{0.05} drawn fiber specimens prepared at the same draw ratios and optimal ATP contents but without acid treatment. Moreover, it is worth noting that the maximal D_{ra} values of the F₁₀₀A_{xM-0.025} as-prepared fiber specimens and the tensile strengths and moduli of the drawn F₁₀₀A_{xM-0.025} fiber specimens reached another maximal value as their ATP nanofibers were treated by 5 M HCl solutions for 60 min. Morphological analyses revealed that more and thinner “micro-fibrils” were present on the etched surfaces of F₁₀₀A_{5M-0.025} fiber specimen than those of F₁₀₀A_{0.025} and F₁₀₀ fiber specimens with the same draw ratios, respectively. The above results suggest that excellent orientation and ultimate tensile properties of UHMWPE fibers can be obtained by ultradrawing the F₁₀₀A_{xM-0.025} as-prepared fibers prepared at the optimal contents of acid treated ATP nanofibers treated with proper condition.

Acknowledgments The authors would like to express their appreciation to the Department of Industrial Technology, Ministry of Economic Affairs (95-EC-17-A-11-S1-057, 96-EC-17-A-11-S1-057, 97-EC-17-A-11-S1-057, 99-EC-17-A-11-S1-155 and 100-EC-17-A-11-S1-155) and National Science Council (NSC 95-2221-E-253 -008 -MY3 and NSC 99-2221-E-011-010-MY3) for support of this work.

Open Access This article is distributed under the terms of the Creative Commons Attribution License which permits any use, distribution, and reproduction in any medium, provided the original author(s) and the source are credited.

References

- Zwijnenburg A, Pennings A (1975) *Colloid Polym Sci* 253:452
- Smith P, Lemstra PJ (1979) *Macromol Chem* 180:2983
- Smith P, Lemstra JP, Pijpers L, Kiel AM (1981) *Colloid Polym Sci* 259:1070
- Ohta T, Okada F (1987) U. S. Patent 4643865
- Ohta T, Okada F, Hayashi M, Mihoichi M (1989) *Polymer* 30:2170
- Furuhata K, Yokokawa T, Ohsawa K, Miyasaka K (1983) *Polym Prepr Jpn* 32:874
- Kanamoto T, Ooki T, Tanaka K, Takeda M (1983) *Polym Prepr Jpn* 32:741
- Smith P, Chanzy HD, Rotzinger BP (1985) *Polym Commun* 26:258
- Chanzy HD, Rotzinger BP, Smith P (1987) Patent WO-8703288
- Smith P, Chanzy HD, Rotzinger BP (1987) *J Mater Sci* 22:523
- Kanamoto T, Ohama T, Tanaka K, Takeda M, Porter RS (1987) *Polymer* 28:1517
- Sawatari C, Okumura T, Matsuo M (1986) *Polymer J* 18:741
- Darras D, Sequela R, Rietsch F (1992) *J Polym Sci Polym Phys Ed* 30:349
- Yeh JT, Lin YL, Fan-Chiang CC (1996) *Macromol Chem Phys* 197:3531
- Yeh JY, Wu HC (1998) *Polym J* 30:1
- Yeh JT, Chang SS, Yen MS (1998) *J Appl Polym Sci* 70:149
- Yeh JT, Chang SS (2000) *J Mater Sci* 35:3227
- Smith P, Lemstra PJ (1980) *J Mater Sci* 15:505
- Yeh JT, Chang SS (2002) *Polym Eng Sci* 42:1558
- Jiang T, Yeh JT, Lin YT, Chen KN (2003) *Polym Eng Sci* 43:1765
- Matsuo M, Sawatari C, Iida M, Yoneda M (1985) *Polym J* 17:1197
- Kanamoto T, Tsurta A, Tanana K, Takeda M, Porter RS (1988) *Macromolecules* 21:470
- Smook J, Pennings AJ (1982) *J Appl Poly Sci* 27:2209
- Prevorsek DC (1982) *Polymer liquid crystals*, Academic Press. pp 357
- Kalb B, Pennings AJ (1980) *Polymer* 21:3
- Wilding MA, Word IM (1978) *Polymer* 19:969
- Smith P, Lemstra PJ (1980) *Polymer* 21:1341
- Kavesh S, Prevorsek DC (1985) U.S. Patent 4536536
- Kavesh S, Prevorsek DC, U.S. Patent 4551296 (1985)
- Kavesh S, Prevorsek DC (1983) U.S. Patent 4413110
- Yeh JT, Wu ZW, Lai YC, Li QC, Zhou HP, Zhou Q, Shu YC, Huang CY (2011) *Pom Eng Sci* 51:2552
- Yeh JT, Wu TW, Lai YC, Zhou HP, Zhou Q, Li QC, Tsai FC, Huang CY, Huang KS, Chen KN (2011) *Polym Eng Sci* 51:687
- Yeh JT, Lin SC, Chen KN, Huang KS (2008) *J Appl Polym Sci* 110:2538
- Yeh JT, Lai YC, Hai L, Yao CS, Chi YN, Kuo SH, Kan NC (2011) *Polym Int* 60:59
- Yeh JT, Du CW, Lin SC, Hsie KH, Chang FC (2008) *J Mater Sci* 43:4892
- Bradley WF (1940) *Am Mineral* 25:405
- Frost RL, Cash GA, Kloprogge JT (1998) *Vib Spectrc* 16(2):173
- Christ, Hathaway CL (1969) *Am Mineral* 54:198
- Drits, Sokolova VA (1971) *Sov Phys Crystallogr* 16:183
- Yamaura K, Tanigami T, Hayashi N, Kosuda KI, Okuda S, Takemura Y, Itoh M, Matsuzawa S (1990) *J Appl Polym Sci* 40:905
- Yeh JT, Wang CK, Hu P, Lai YC, Hai L, Tsai FC (2012) *Polym Int* 6:982
- Kajiwarra K, Mcintyre JE (1994) *Advanced fiber spinning technology*. Woodhead Publishing, Cambridge, p 174
- Hoffman JD, Miller RL (1997) *Polymer* 38:3151
- Hoffman JD, Weeks JJ (1962) *J Res Natl Bur Stand* 66:13
- Xiao H, Zhang Y, An S, Jia G (1996) *J Appl Polym Sci* 59:931
- Zhao L, Du Q, Jiang G, Guo SJ (2007) *J Polym Sci Part B: Polym Phys* 45:16
- Boudriche L, Calvet R, Hamdi B, Balard H (2011) *Colloids Surf A: Physi* 45:392
- Ohta T (1983) *Polym Eng Sci* 23:697
- Hoogsteen W, ten Brinke G, Pennings AJ (1988) *Colloid Polym Sci* 266:1003